Electrochimica Acta 110 (2013) 208–213

Contents lists available at ScienceDirect

Electrochimica Acta

journal homepage: www.elsevier.com/locate/electacta

P2-type layered $Na_{0.45}Ni_{0.22}Co_{0.11}Mn_{0.66}O_2$ as intercalation host material for lithium and sodium batteries

Daniel Buchholz, Luciana Gomes Chagas, Martin Winter [1], Stefano Passerini *, [1]

MEET Battery Research Centre, Institute of Physical Chemistry, University of Münster, Corrensstr. 46, 48149 Münster, Germany

ARTICLE INFO

Article history:
Received 30 November 2012
Received in revised form 19 February 2013
Accepted 23 February 2013
Available online 4 March 2013

Keywords:
Cathode material
Layered
High stability
Sodium and lithium batteries
Intercalation

ABSTRACT

Herein is reported the electrochemical performance of $Na_{0.45}Ni_{0.22}Co_{0.11}Mn_{0.66}O_2$ as cathode material for lithium and sodium batteries. The material is able to reversibly accommodate both cation species but reveals a much better electrochemical performance towards Na-ion intercalation. Upon galvanostatic cycling for 100 cycles a much higher capacity retention (82% vs. Na, 61% vs. Li) and higher coulombic efficiency (99.5% vs. Na, 98.5% vs. Li) are shown by the sodium-based system. The worse electrochemical performance of the lithium-based system can be explained by the much higher irreversibility of the Mn^{3+}/Mn^{4+} redox process.

1. Introduction

The sodium-ion technology is currently attracting interest since it offers cost saving aspects combined with suitable energy densities and electrochemical performances. The high abundance and wide spread availability of sodium in contrast to lithium [1] combined with the possibility of using aluminium as anode current collector (sodium does not alloy with it [2]) represent interesting cost cutting potential with respect to today's lithium-ion technology. These are especially important if a rapid upscaling of lithium-ion battery (LIB) production will take place led by the use of lithium-ion batteries for electric vehicles. In fact, this could yield further problems associated with not suitable lithium mining. Sodium-ion batteries might then assist to counter the possible lithium shortage and increasing prices [3] by replacing LIBs in fields where the energy density is not as restrictive as for electromobility, e.g. stationary energy storage or portable electronic devices [4–6]. In fact, recent works have demonstrated that sodium-ion batteries own good electrochemical performance, superior to that of other secondary batteries except for lithium-ion batteries [7–11].

Recent investigations have shown that especially 2D-layered transition metal oxides are promising candidates as cathodes materials in sodium-ion batteries. For the development and design of layered cathode materials three major trends are visible here:

(a) Replacing toxic and expensive transition metals like in $NaCrO_2$ [7] by environmentally friendly and cheaper Mn-based materials, such as P2-$Na_{0.67}[Fe_{0.5}Mn_{0.5}]O_2$ or $Na[Ni_{0.33}Fe_{0.33}Mn_{0.33}]O_2$ [8,9]; (b) taking advantage of transition metal intermixing, like in $NaNi_{1/3}Mn_{1/3}Co_{1/3}O_2$ [10], in order to combine the several advantages of the different metals while erasing the drawbacks and challenges related to the pure oxides and (c) stabilizing the sodium layered oxides by implementing smaller cations inside, such as $Na_{1.0}Li_{0.2}Ni_{0.25}Mn_{0.75}O_\delta$ [11].

In a previous work we showed that combining the strategies of transition metal intermixing with the implementation of smaller cations inside the material (via a water treatment) is a promising method to improve the stability of layered sodium-based cathode materials. $Na_{0.45}Ni_{0.22}Co_{0.11}Mn_{0.66}O_2$ synthesized by a simple solid state synthesis in air revealed an extraordinary cycling performance with an average coulombic efficiency of 99.7% [12]. The details of the structural characterization and the effect of the water treatment on the performance of $Na_{0.45}Ni_{0.22}Co_{0.11}Mn_{0.66}O_2$ cathode material are described in our previous work. Evidences of protons being present in the material were reported in this work, however, the quantification is not achieved yet.

Layered cathode materials are also well known and established for lithium ion batteries [13], however some work reports the insertion of other cations. Bruce and colleagues investigated the behaviour of various host materials towards the chemical intercalation of different cation species, like Na^+, Mg^{2+} and Zn^{2+} in layered WO_2Cl_2 and layered TiS_2 [14–16]. In addition, the chemical ion-exchange of sodium by lithium ions was a common procedure to obtain the corresponding lithium containing layered material [17].

* Corresponding author. Tel.: +49 251 8336725; fax: +49 251 8336797.
E-mail address: stefano.passerini@uni-muenster.de (S. Passerini).
[1] ISE member.

0013-4686/$ – see front matter © 2013 Elsevier Ltd. All rights reserved.
http://dx.doi.org/10.1016/j.electacta.2013.02.109

Following this idea, our basic approach was the use of a P2-type, sodium based host structure, as an intercalation host material for the smaller lithium cations, whereby the sodium cations should be replaced electrochemically. The development of a universal intercalation host material able to reversibly accommodating different alkali metal species would allow the implementation of one cathode material in different kinds of secondary ion batteries.

Herein, we present the investigation on the electrochemical performance of $Na_{0.45}Ni_{0.22}Co_{0.11}Mn_{0.66}O_2$ as cathode material for lithium and sodium batteries. The objective of the work was to check the compatibility and suitability of the layered P2-type $Na_{0.45}Ni_{0.22}Co_{0.11}Mn_{0.66}O_2$ cathode material as host structure for lithium and sodium ions.

2. Experimental

The material was synthesized by a solid-state reaction method from sodium hydroxide (NaOH, Aldrich >98%) and a manganese–nickel–cobalt hydroxide precursor. The latter was prepared by co-precipitating an aqueous solution of the three metal acetate salts (Mn, Ni, and Co; Aldrich >98%, weight ratio of 66:22:11) with sodium hydroxide (50% excess). After extensive rinsing with distilled water, the precipitate was dried under vacuum at 120 °C overnight. The dried material was then dispersed in an aqueous solution of sodium hydroxide (0.63 eq. of NaOH per mole of $Ni_{0.22}Co_{0.11}Mn_{0.66}(OH)_2$). Water was slowly removed by rotary evaporator. After drying and grinding, the mixture was annealed in air at 500 °C for 5 h, and then, as a pellet, at 800 °C for 6 h, using an open-air muffle oven. Afterwards the material was grinded, screened over a 45 μm sieve and, finally, stored under inert atmosphere. For the water treatment about 1 g of the as-prepared material was stirred in 20 mL of distilled water (at 25 °C) for 5 min. The suspension was then filtered and washed with 80 mL of distilled water, dried at 120 °C in air for 24 h and finally stored under inert atmosphere.

2.1. Characterization

Electrodes were prepared by casting the slurry, composed of 85 wt.% active material, 10 wt.% Super C65 (TIMCAL), and 5 wt.% PVDF (6020 Solef®, Arkema Group), onto Al foil. The active material mass loading in the electrodes was about 2 mg cm^{-2}.

Sodium or lithium metals were used as counter and reference electrodes for the corresponding half cells. Lithium electrodes were punched out of lithium foil (Rockwood Lithium). Sodium electrodes were made from sodium chunks (99.8%, Acros Organics), which were rolled, pressed, and finally punched on the current collector. The cathode electrodes were assembled into Swagelok cells using either 1 M $LiPF_6$ in EC:DMC = 1:1 (Merck, LP30) or 0.5 M $NaPF_6$ (99%, ABCR) in PC (UBE, Japan) as the electrolyte solution for the lithium or sodium cell, respectively. Cells were cycled galvanostatically at different constant current rates (nominal capacity = 122 mAh g^{-1}, 1 C = 122 mA g^{-1}) between 4.3 V and 2.1 V (vs. Na/Na^+) or 4.6 V and 2.4 V (vs. Li/Li^+) at 20 °C using Maccor series 4000 battery tester (USA). All experiments, including synthesis, were duplicated, at least twice, to check reproducibility.

3. Results and discussion

P2-type $Na_{0.45}Ni_{0.22}Co_{0.11}Mn_{0.66}O_2$ cathode material has been synthesized via co-precipitation method and a two step solid state process. The chemical composition has been verified via ICP-OES analysis. Details of the synthesis and the structural characterization can be found in our previous work [12].

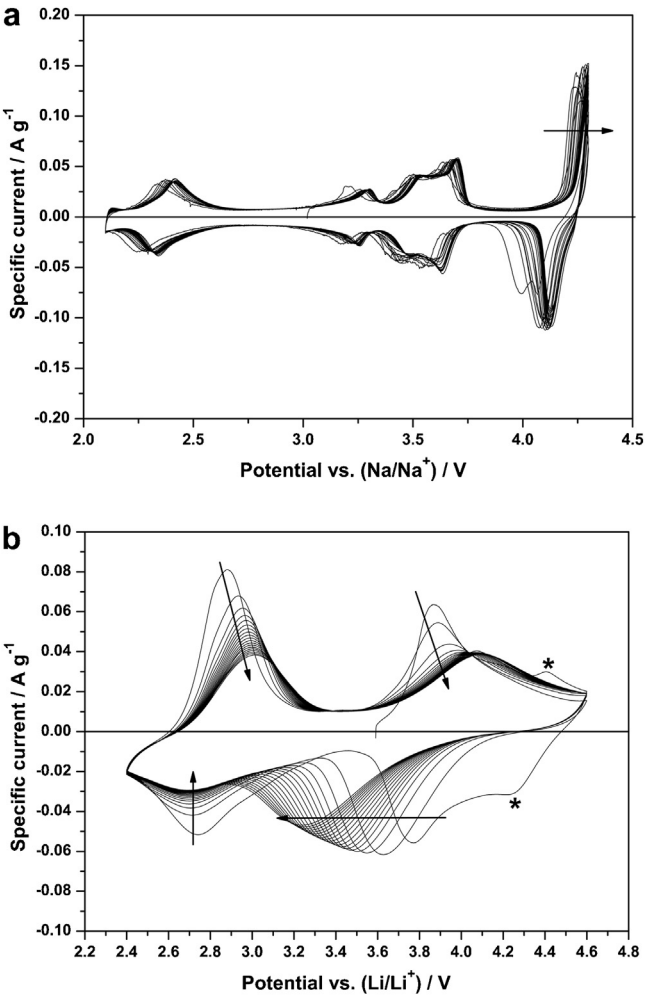

Fig. 1. Cyclic voltammograms (cycles 1–20) of $Na_{0.45}Ni_{0.22}Co_{0.11}Mn_{0.66}O_2$ versus (a) sodium and (b) lithium. Cut-off limits: 4.3–2.1 V (vs. Na/Na^+); 4.6–2.4 V (vs. Li/Li^+). Reference and counter electrodes: Na or Li. Electrolyte: 0.5 M $NaPF_6$ in PC; 1 M $LiPF_6$ in EC:DMC = 1:1. Scan rate of 0.1 mV/s. Temperature: 20 °C ± 2 °C.

Cyclic voltammetry was initially performed on $Na_{0.45}Ni_{0.22}Co_{0.11}Mn_{0.66}O_2$ to obtain general information about the electrochemical processes taking place in both (Li, Na) systems (Fig. 1).

The cyclic voltammograms indicate that the electrochemical intercalation behaviour of Na^+ and Li^+-ions in $Na_{0.45}Ni_{0.22}Co_{0.11}Mn_{0.66}O_{2-\delta}$ is very different.

For the sodium-based system (Fig. 1a) five anodic and five cathodic current peaks can be observed, located at about 4.2 V, 3.7 V, 3.5 V, 3.3 V and 2.4 V and at 4.1 V, 3.6 V, 3.4 V, 3.2 V and 2.3 V, respectively. The four anodic and four cathodic peak occurring within the potential range 2.1–3.8 V (vs. Na/Na^+) does not change upon consecutive voltammetric cycles. Only minor shift of these peaks is observed within this potential range, thus indicating the high stability and reversibility of these Na^+ ion intercalation processes. The anodic and cathodic peaks at higher potentials (>4.0 V) exhibit slight more marked differences in terms of current and position, which indicate this to be the less reversible electrochemical process. The current intensity of the charge peak is, in fact, about 0.17 A g^{-1}, i.e. higher than that of the broad corresponding discharge peak, showing an intensity of about 0.11 A g^{-1}.

The peak assignment of the sodium system can partially be done based on literature [18,19]. The anodic peak at high potentials of about 4.2 V vs. Na/Na^+ is related with the quasi-reversible P2-type to O2-type phase transition occurring at low sodium content in the

material. This phase change occurs because the octahedral coordination geometry generated by the oxygen layer movement inside the material is energetically stable, it leads to a reduced repulsion of the electron shells of the oxygen anions, with respect to the trigonal prismatic coordination. In the subsequent discharge process (sodium intercalation) the P2-type structure is built again since the sodium cations are more stable in this latter structure than in the octahedral coordination geometry.

The peaks in the potential range 3.1–3.8 V are related to the different staging and alignment of the sodium layers in the material and (de-)insertion of the sodium cations from it [18,19]. The peak couple at lower potentials (≤2.4 V) is not reported in literature for similar sodium-based layered cathode materials, so far. Based on the potential at which the electrochemical process is taking place, this feature could be associated to the Mn^{3+}/Mn^{4+} redox reactions.

On the other hand, the cyclic voltammogram of the lithium cell shows a poor stability of the electrochemical lithiation processes (Fig. 1b). Two anodic and cathodic broad peaks are observed in the lithium-based system, which is initially located at about 2.9 V and 3.9 V and about 2.7 V and 3.8 V, respectively. In the first cycle an additional peak couple is observed at 4.4 V (charge) and 4.3 V (discharge). However, these features disappear in the second cycle, already. During the consecutive cyclic voltammetries the anodic peak at low potentials (about 2.9 V) shifts to 3.0 V and continuously decreases in intensity (from 0.08 A g^{-1} to 0.04 A g^{-1}). The second anodic peak located at about 3.9 V also shifts to 4.1 V upon cycling and exhibits a rather constant intensity of 0.04 A g^{-1} (after an initial fading from 0.06 A g^{-1}). On the cathodic sweeps the anodic peak at high potential (3.75 V) broadens and, additionally, shifts drastically towards lower potentials (3.2 V). The intensity of this peak decreases from 0.06 A g^{-1} to 0.04 A g^{-1}, as well. On the other hand, the peak at 2.7 V does not shift towards lower values but its intensity decreases from 0.05 A g^{-1} to 0.03 A g^{-1}.

Taking the potential difference of about 300 mV between lithium and sodium quasi-reference electrodes, the high potential peak appearing only during the first charge process is to be related with the high potential peak at which the P2-O2 phase transition occurs for the sodium cell. In pristine $Na_{0.45}Ni_{0.22}Co_{0.11}Mn_{0.66}O_2$, in fact, material only sodium cations are present, which are still coordinated trigonal prismatic. Towards the end of the first charge, i.e. at low sodium contents the phase transition to the O2-type occurs, which causes the appearance of the peak in the first anodic sweep. The peak at 4.3 V in the first cathodic sweep corresponds to the lithium intercalation in the cathode structure. This peak is associated with a further gliding of the transition metal layers leading to the formation of a stacked fault O2-type structure rather than the original P2 structure. This phenomenon is already known for layered, lithium-based cathode materials synthesized via chemical ion exchange from sodiated precursors [20,21]. These compounds, in fact, adopt a T2-type or a stacked fault O2-type structure when a certain amount (e.g. 1/12 eq.) of nickel in the transition metal layer was replaced by cobalt.

However, starting from the second voltammetric cycle only two current peaks are visible during each anodic and cathodic sweeps. The peak couple at high potentials certainly correlates with the redox reaction of Ni^{2+}/Ni^{4+} and, probably, also of Co^{3+}/Co^{4+}, which is redox active at high potentials (about 4.4 V vs. Li) [20,22]. The peak couple at lower potentials (about 2.7–2.8 V) instead is caused by the redox reaction of Mn^{3+}/Mn^{4+} [20]. The presence of this peak couple also confirms the assignment of the low potential peak couple observed at about 2.4 V (vs. Na) for the sodium-based system.

Finally, the comparison of the voltammograms recorded for the Na- and Li-based cells indicates that the host structure exhibits a much higher stability towards (de-)intercalation of sodium. In the Li-system, in fact, the evolution of large overpotentials is observed,

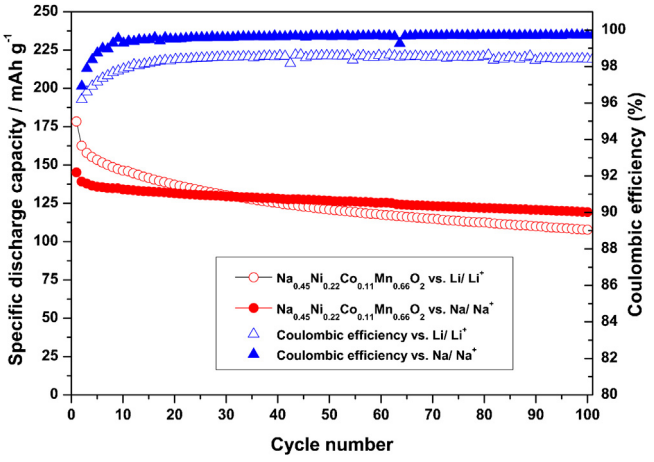

Fig. 2. Comparison of the specific discharge capacities detected upon galvanostatic cycling (100 cycles) of $Na_{0.45}Ni_{0.22}Co_{0.11}Mn_{0.66}O_2$ at 0.1 C (12 mA g^{-1}) versus lithium (hollow markers) and sodium (filled markers). Cut-off limits: 4.3–2.1 V (vs. Na/Na^+); 4.6–2.4 V (vs. Li/Li^+). Reference and counter electrodes: Na or Li. Electrolyte: 0.5 M $NaPF_6$ in PC; 1 M $LiPF_6$ in EC:DMC = 1:1. Temperature: 20 °C ± 2 °C.

finally resulting in the shift and strong intensity decrease of the peaks upon cycling.

To validate the assumption regarding the electrochemical stability, galvanostatic cycling tests were performed on $Na_{0.45}Ni_{0.22}Co_{0.11}Mn_{0.66}O_2$ (Fig. 2).

At a first glance it is obvious that the cycling behaviour of $Na_{0.45}Ni_{0.22}Co_{0.11}Mn_{0.66}O_2$ is more stable in the sodium cell than in the lithium cell, although the first discharge capacity is higher in the latter (178 mAh g^{-1}, corresponding to 0.65 eq. of lithium insertion) than in the former (145 mAh g^{-1}, corresponding to 0.54 eq. of sodium insertion). From the stoichiometry of the layered $Na_{0.45}Ni_{0.22}Co_{0.11}Mn_{0.66}O_2$ material, assuming the typical oxidation states of Ni^{2+} and Co^{3+}, a maximum (de-)insertion of 0.53 eq. is calculated when both nickel and cobalt are considered redox active. This value corresponds to a much lower capacity than that detected for the lithium cell and confirms that manganese is also redox active with respect to lithium (de-)insertion, as indicated by the cyclic voltammetry results presented above [23].

After the first cycle a capacity fading can be observed for both systems, which takes place until the 10th cycle, and leads to a discharge capacity of 146 mAh g^{-1} for the lithium cell and 134 mAh g^{-1} for the sodium cell. Thereby, the efficiency of both systems is increasing from 96.2% to 97.8% (Li) and 96.9% to 99.2% (Na) from the 2nd to the 10th cycle. Afterwards, the efficiency of the lithium cell slightly increases to about 98.5% whereas the sodium cell achieves the extraordinary coulombic efficiency of 99.6%. This difference in coulombic efficiency underlines the overall cycling behaviour of $Na_{0.45}Ni_{0.22}Co_{0.11}Mn_{0.66}O_2$ in the two systems (Na and Li). Upon cycling the lithium cell exhibits a steady capacity fading whereas the sodium cell exhibits a stable cycling behaviour. As a result, starting from the 30th cycle, the sodium cell delivers higher specific discharge capacities than the lithium cell. At the 100th cycle discharge capacities of about 108 mAh g^{-1} for the lithium cell and 119 mAh g^{-1} for the sodium cell are detected. These values correspond to a capacity retention of only 60.6% (capacity loss of 0.70 mAh g^{-1} per cycle) for the former and the extraordinary value of 82.1% (capacity loss of 0.26 mAh g^{-1} per cycle) for the latter. The different cycling behaviour is explained by the evolution of the potential profiles recorded for the lithium and sodium cells in (Fig. 3).

The first charge capacity is for both cells about 120 mAh g^{-1}, corresponding to 0.44 eq. of sodium removed. This is in a very good agreement with the full desodiation of the cathode material

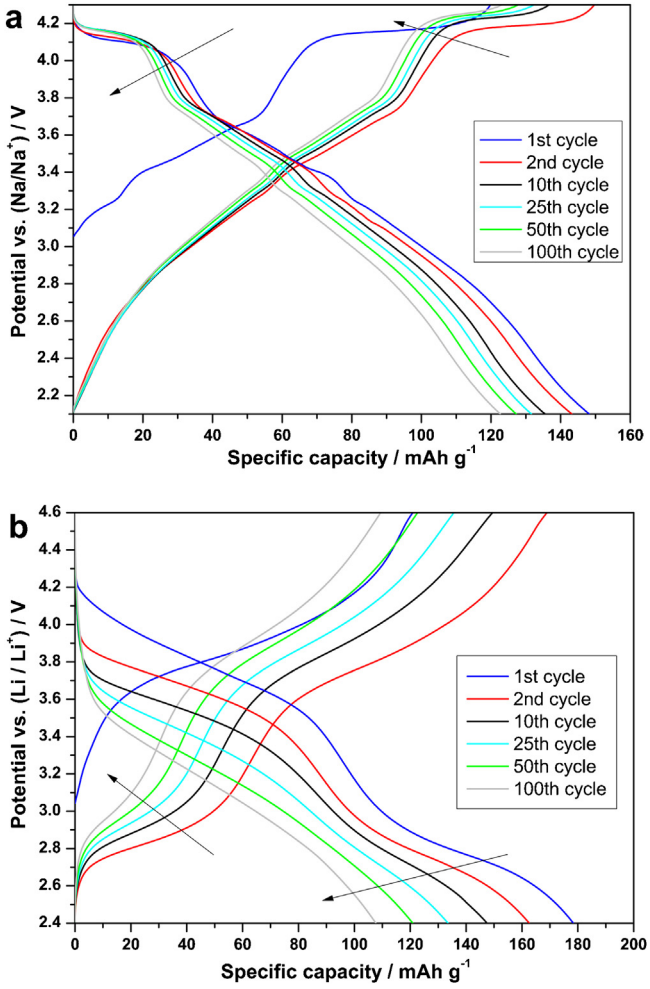

Fig. 3. Potential versus capacity profiles of $Na_{0.45}Ni_{0.22}Co_{0.11}Mn_{0.66}O_2$ during the 1st, 2nd, 10th, 25th, 50th and 100th cycle at 0.1 C (12 mA g^{-1}) versus sodium (a) and lithium (b). Cut-off limits: 4.3–2.1 V (vs. Na/Na^+); 4.6–2.4 V (vs. Li/Li^+). Reference and counter electrodes: Na or Li. Electrolyte: 0.5 M $NaPF_6$ in PC; 1 M $LiPF_6$ in EC:DMC = 1:1. Temperature: 20 °C ± 2 °C.

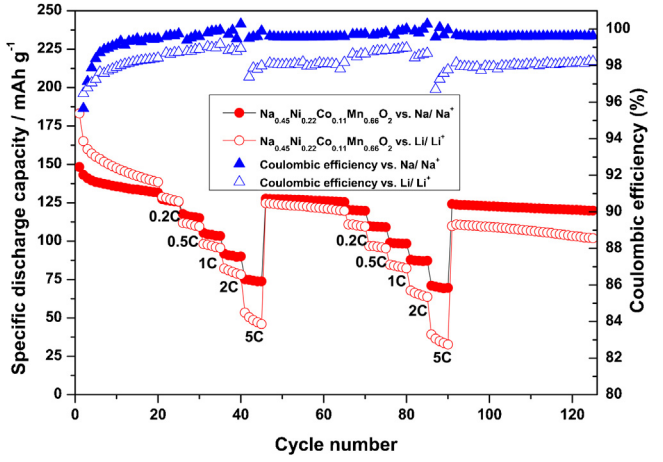

Fig. 4. Comparison of the specific discharge capacities detected upon galvanostatic cycling of $Na_{0.45}Ni_{0.22}Co_{0.11}Mn_{0.66}O_2$ versus lithium (hollow markers) or sodium (filled markers) at 0.1 C (12 mA g^{-1}) for 125 cycles. Cycles 21 through 45 and 65 through 90 illustrate the behaviour during the C-rate test performed at 0.2 C (24 mA g^{-1}), 0.5 C (61 mA g^{-1}), 1 C (122 mA g^{-1}), 2 C (244 mA g^{-1}) and 5 C (610 mA g^{-1}). Cut-off limits: 4.3–2.1 V (vs. Na/Na^+); 4.6–2.4 V (vs. Li/Li^+). Reference and counter electrodes: Na or Li. Electrolyte: 0.5 M $NaPF_6$ in PC; 1 M $LiPF_6$ in EC:DMC = 1:1. Temperature: 20 °C ± 2 °C.

independent on the kind of cell (Li or Na). In the subsequent cycle, however, the discharge capacities for both cells are higher. This additional capacity is due to the reduction of Mn^{4+} to Mn^{3+}.

The potential profile of the sodium cell (Fig. 3a) shows a cascade-like behaviour typical of layered sodium-based cathode materials. From the different slopes of the potential profile, four features can be identified for the charge and discharge processes, which are consistent with cyclic voltammetry. The slight fading of the sodium cell can mostly be attributed to the shortening of the high potential plateaus, especially that at 4.1 V, which is exhibiting about 35 mAh g^{-1} in the first discharge process, but only about 20 mAh g^{-1} in the 100th discharge cycle. This is expected since this plateau is associated with the phase transition from the P2- to the O2-type, which is the less reversible process. Additionally, the sloppy plateau located at about 3.6 V is slightly fading, whereas the features below 3.2 V show nearly no change in overpotentials (see the overlapping charge curves up to 3.2 V). Overall, only a minor evolution of overpotentials can be observed for the sodium system, underlining the extraordinary cycling performance for a first generation, lab-scale material.

In contrast, the potential profile evolution of the lithium-based system is confirming the worse cycling performance depicted in Fig. 2. Two plateaus are seen at about 4.0 V and 2.9 V during the charge process and 3.5 V and 2.7 V for the discharge process. The plateau at higher potential strongly shifts upon cycling of about 300 mV towards higher potentials in the charge process and about 800 mV in the discharge process. This strong shift of the voltage plateau is caused by the evolution of a large activation and ohmic overpotential upon cycling. Compared to the huge overpotential evolution only a minor capacity fade of the high potential plateau can be observed. The capacity delivered by the material within the range 4.6–3.6 V decreases from 90 mAh g^{-1} only to 70 mAh g^{-1}, indicating the partial reversibility of the electrochemical process related with the redox reaction of Ni. On the contrary, the plateau at lower potentials, related with the redox reaction of manganese, exhibits less overpotential evolution (e.g. 200 mV for the charge process) but is clearly causing the capacity fade upon cycling. For the charge process initially 60 mAh g^{-1} are delivered within the potential range 2.4–3.0 V, which is further decreasing to only 20 mAh g^{-1} in the 100th cycle.

Such a large capacity fading is explained by the poor stability of Mn^{3+}, which is known to be a Jahn–Teller distorted $3d^4$ ion. The formation of Mn^{3+} results in large structural distortions of the crystalline structure while Mn^{3+} undergoes the disproportion reaction leading to Mn^{4+} and Mn^{2+}. The latter is known to easily dissolve in the electrolytic solution, thus leading to a constant degradation of the active material. Further, it is known that materials synthesized via ion-exchange exhibit an even higher amount of Mn^{3+} [24].

The overall performance of $Na_{0.45}Ni_{0.22}Co_{0.11}Mn_{0.66}O_2$ as cathode material for lithium and sodium batteries was also evaluated by a combined constant current cycling and current-rate test (Fig. 4).

As indicated by the previous results, P2-type $Na_{0.45}Ni_{0.22}Co_{0.11}Mn_{0.66}O_2$ exhibits a much better cycling performance compared to the lithium one, although the former cell exhibits a lower discharge capacity (148 mAh g^{-1}) than the latter (183 mAh g^{-1}) in the first cycle. Both systems reveal again a higher capacity decay within the first ten cycles. Discharge capacities of 135 mAh g^{-1} for the sodium-cell and 147 mAh g^{-1} for the lithium cell are detected in the 10th cycle. The efficiencies increase from 95.7% in the 2nd cycle to 99.2% in the 10th cycle for the sodium cell and from 96.5% in the 2nd to 97.9% in the 10th cycle for the lithium cell. For the sodium system the efficiencies are then increasing to values higher than 99.6% and further constant for the whole galvanostatic cycling and rate performance test at different current

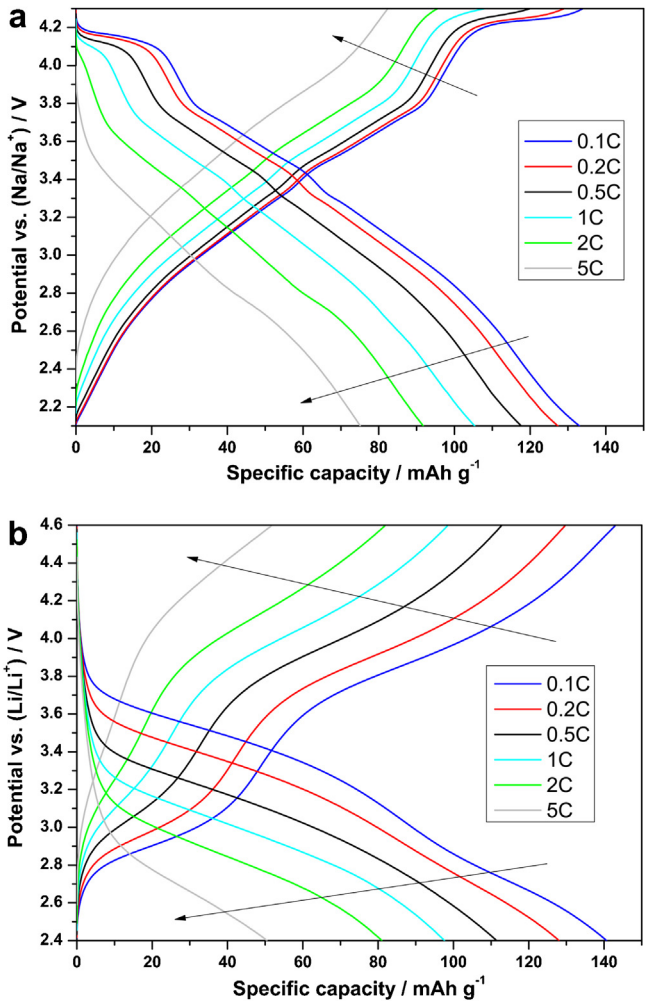

Fig. 5. Potential vs. capacity profiles of $Na_{0.45}Ni_{0.22}Co_{0.11}Mn_{0.66}O_2$ during the C-rate test performed at 0.1 C (12 mA g^{-1}), 0.2 C (24 mA g^{-1}), 0.5 C (61 mA g^{-1}), 1 C (122 mA g^{-1}), 2 C (244 mA g^{-1}) and 5 C (610 mA g^{-1}) versus sodium (a) and lithium (b). Cut-off limits: 4.3–2.1 V (vs. Na/Na^+); 4.6–2.4 V (vs. Li/Li^+). Reference and counter electrodes: Na or Li. Electrolyte: 0.5 M $NaPF_6$ in PC; 1 M $LiPF_6$ in EC:DMC = 1:1. Temperature: 20 °C ± 2 °C.

rates. On the other hand, the efficiencies for the lithium system are generally lower.

Additionally, the rate capability of the sodium system is better than that of the lithium system. In fact, the specific discharge capacities at 0.2 C (24 mA g^{-1}), 0.5 C (61 mA g^{-1}), 1 C (122 mA g^{-1}), 2 C (244 mA g^{-1}) and 5 C (610 mA g^{-1}) are, respectively, 127 mAh g^{-1}, 117 mAh g^{-1}, 105 mAh g^{-1}, 92 mAh g^{-1} and 75 mAh g^{-1} for the sodium system and 129 mAh g^{-1}, 112 mAh g^{-1}, 98 mAh g^{-1}, 82 mAh g^{-1} and 53 mAh g^{-1} for the lithium system.

The reasons for the superior rate capability of the sodium system can be understood by observing potential profiles at the different current rates (Fig. 5).

For the sodium system, higher charge current rates mostly lead to the shortening of the high potential plateau, which completely disappears at current rates higher than 2 C. This plateau is expected to be the rate-determining step for cycling at higher current rates since it is related with the energetically hindered P2- to O2-type phase transition. For the lithium system, however, it is the low voltage plateau, which shortens upon increasing rates to disappear when current rates higher than 2 C are used.

The most pronounced difference between the potential profiles of Na- and Li-based cells is the activation overpotential especially upon ion intercalation. In fact, it has only a minor influence on the sodium system, whereas for the lithium based system the activation overpotential for lithium insertion increases about 800 mV for a 50-fold current density increase. The electrode activation polarization is the cause for the worse overall electrochemical performance of the lithium system.

4. Conclusions

The electrochemical investigations revealed that layered P2-type $Na_{0.45}Ni_{0.22}Co_{0.11}Mn_{0.66}O_2$ material is able to reversibly accommodate sodium and lithium cations. However, the cycling and rate performance tests revealed a much better performance for the sodium-based system compared with the lithium one. This difference is mainly attributed to the evolution of large overpotentials for the lithium based system and to the fading of the plateau at 2.7 V (vs. Li) upon cycling, which is related with the redox reaction between Mn^{3+} and Mn^{4+}. In contrast this electrochemical process is very reversible for the sodium-based system. Therefore, we propose a different extent of the Jahn–Teller effect in the two cell systems as the main reason for the different electrochemical performance.

Acknowledgements

D.B. would like to thank VW and Rockwood Lithium for the financial support. L.C. would like to acknowledge the Conselho Nacional de Desenvolvimento Científico e Tecnológico (CNPq, Brazil) for the financial support.

References

[1] A.F. Hollemann, E. Wiberg, N. Wiberg, Lehrbuch der Anorganischen Chemie, de Gruyter, Berlin/New York, 1985.
[2] H. Baker, H. Okamoto, ASM Handbook Alloy phase diagrams, vol. 3, ASM International, USA, 1992.
[3] J.M. Tarascon, Is lithium the new gold? Nature Chemistry 2 (2010) 510.
[4] S.-W. Kim, D.-H. Seo, X. Ma, G. Ceder, K. Kang, Electrode materials for rechargeable sodium-ion batteries: potential alternatives to current lithium-ion batteries, Advance Energy Materials 2 (2012) 710.
[5] V. Palomares, P. Serras, I. Villaluenga, K.B. Hueso, J. Carretero-González, T. Rojo, Na-ion batteries, recent advances and present challenges to become low cost energy storage systems, Energy & Environmental Science 5 (2012) 5884.
[6] B. Dunn, H. Kamath, J.M. Tarascon, Electrical energy storage for the grid: a battery of choices, Science 334 (2011) 928.
[7] S. Komaba, C. Takei, T. Nakayama, A. Ogata, N. Yabuuchi, Electrochemical intercalation activity of layered $NaCrO_2$ vs. $LiCrO_2$, Electrochemistry Communications 12 (2010) 355.
[8] N. Yabuuchi, M. Kajiyama, J. Iwatate, H. Nishikawa, S. Hitomi, R. Okuyama, R. Usui, Y. Yamada, S. Komaba, P2-type $Na_x[Fe_{1/2}Mn_{1/2}]O_2$ made from earth-abundant elements for rechargeable Na batteries, Nature Materials 11 (2012) 512.
[9] D. Kim, E. Lee, M. Slater, W. Lu, S. Rood, C.S. Johnson, Layered $Na[Ni_{1/3}Fe_{1/3}Mn_{1/3}]O_2$ cathodes for Na-ion battery application, Electrochemistry Communications 18 (2012) 66.
[10] M. Sathiya, K. Hemalatha, K. Ramesha, J.M. Tarascon, A.S. Prakash, Synthesis, structure, and electrochemical properties of the layered sodium insertion cathode Material: $NaNi_{1/3}Mn_{1/3}Co_{1/3}O_2$, Chemistry of Materials 24 (2012) 1846.
[11] D. Kim, S.-H. Kang, M. Slater, S. Rood, J.T. Vaughey, N. Karan, M. Balasubramanian, C.S. Johnson, Enabling sodium batteries using lithium-substituted sodium layered transition metal oxide cathodes, Advanced Energy Materials 1 (2011) 333.
[12] D. Buchholz, A. Moretti, R. Kloepsch, S. Nowak, V. Siozios, M. Winter, S. Passerini, Towards Na-ion batteries – synthesis and characterization of a novel high capacity Na-ion intercalation material, Chemistry of Materials 25 (2013) 142.
[13] M.S. Whittingham, Lithium batteries and cathode materials, Chemical Reviews 104 (2004) 4271.
[14] P.G. Bruce, J. Nowinski, Sodium Intercalation into WO_2Cl_2, Journal of Solid State Chemistry 89 (1990) 202.
[15] P.G. Bruce, F. Krok, P. Lightfoot, J.L. Nowinski, Multivalent cation intercalation, Solid State Ionics 53–56 (1992) 351.
[16] P.G. Bruce, F. Krok, J. Nowinski, V.C. Gibson, K. Tavakkoli, Chemical intercalation of magnesium into solid hosts, Journal of Materials Chemistry 1 (1991) 705.

[17] A.D. Robertson, A.R.A., A.J. Fowkes, P.G. Bruce, $Li_x(Mn_{1-2y}Co_y)O_2$ intercalation compounds as electrodes for lithium batteries: influence of ion exchange on structure and performance, Journal of Materials Chemistry 11 (2001) 113.
[18] Z. Lu, J.R. Dahn, The effect of Co substitution for Ni on the structure and electrochemical behavior of T2 and O2 structure $Li_{2/3}[Co_xNi_{1/3-x}Mn_{2/3}]O_2$, Journal of the Electrochemical Society 14 (2001), A237.
[19] Z. Lu, J.R. Dahn, In Situ X-Ray Diffraction Study of P2-$Na_{2/3}[Ni_{1/3}Mn_{2/3}]O_2$, Journal of the Electrochemical Society 148 (2001) A1225.
[20] Z. Lu, R.A. Donaberger, C.L. Thomas, J.R. Dahn, T2 and O2 $Li_{2/3}[Co_xNi_{1/3-x/2}Mn_{2/3-x/2}]O_2$ electrode materials, Journal of the Electrochemical Society 149 (2002) A1083.
[21] J.M. Paulsen, R.A. Donaberger, J.R. Dahn, Layered T2-O6-O2- and P2-Type $A_{2/3}[M'^{2+}{}_{1/3}\ M^{4+}{}_{2/3}]O_2$ Bronzes A = Li, Na; M′ = Ni, Mg; M = Mn, Ti, Chemistry of Materials 12 (2000) 2257.
[22] J. Li, Z.R. Zhang, X.J. Guo, Y. Yang, The studies on structural and thermal properties of delithiated $Li_xNi_{1/3}Co_{1/3}Mn_{1/3}O_2 (0 < x \leq 1)$ as a cathode material in lithium ion batteries, Solid State Ionics 177 (2006) 1509.
[23] Z. Lu, J.R. Dahn, Can all the lithium be removed from T2-$Li_{2/3}[Ni_{1/3}Mn_{2/3}]O_2$? Journal of the Electrochemical Society 14 (2001), A710.
[24] A.D. Robertson, A.R. Armstrong, A.J. Paterson, M.J. Duncan, P.G. Bruce, Non-stoichiometric layered $Li_xMn_yO_2$ intercalation electrodes—a multiple dopant strategy, Journal of Materials Chemistry 13 (2003) 2367.